MEASUREMENT OF DRAG REDUCTION IN DILUTE POLYMER SOLUTION USING TRIBOELECTRIC EFFECT

BLAISE NSOM* AND NOUREDDINE LATRACHE

Université de Bretagne Occidentale, Institut de Recherche Dupuy de Lôme, Rue de Kergoat, 29238 Brest Cedex 3, France

*Corresponding author: blaise.nsom@univ-brest.fr

Received: 20.12.2017, Final version: 25.3.2018

ABSTRACT:

In this paper, we present a novel method we have developed for measuring the drag reduction in a dilute polymer solution, based on the triboelectricity phenomenon. The presence of a small quantity of polymer with high molecular density in a liquid decreases the friction of the liquid on solid walls. This property defines drag reduction. The friction itself produces electricity in the liquid known as triboelectricity. In this work, we show that drag reduction can be measured by measuring the triboelectric voltage in the solvent and in the polymer solution. The method was tested on well characterized dilute solution of polyethylene oxide (PEO) and the results obtained agree qualitatively well with those available in the literature, notably showing that for given flow rate, drag reduction by PEO increases with polymer concentration until reaching a plateau. Also, for given concentration, drag reduction increases with flow rate in the range of concentration and flow rate tested. More generally, a similar behavior is expected for any polymer solution obeying the power-law rheological model.

KEY WORDS:

Drag reduction, hydroelectric model, insulating liquid, polymer solution, power-law, triboelectricity

1 INTRODUCTION

Liquid in a pipeline generally flows according to the turbulent regime and, therefore, generates high-energy dissipation due to high friction at the solid walls [1]. To reduce process costs, engineers need to reduce energy dissipation using drag reduction (DR). Two types of DR exist, known as active and passive [2]. Active DR relies on the introduction of a small quantity of an appropriate additive to reduce the drag coefficient. These external agents can be polymers, surfactants or fibers [3–8]. Passive techniques consist in modifying the geometry of the surface (coatings and riblets) to alter the flow characteristics. However, these passive techniques are much less efficient than the active ones [9].

Some explanations have been proposed for the drag reduction phenomenon. Shefty and Solomon [10] noted the presence of aggregates in freshly prepared solutions and the drag reduction was attributed to the destruction of these aggregates. Virk [11] proposed a modification of the velocity profile in ducts, introducing an elastic sublayer between the usual Newtonian viscous sublayer and the logarithmic velocity profile. As the elastic sublayer increases, the logarithmic velocity profile decreases and the DR increases to its maximum

value. Polyethylene oxide (PEO), which we chose to use as the additive in this study, has been much studied theoretically, numerically and experimentally for commercial applications such as fire prevention and marine propulsion because of its low cost, high availability, as well as its linear and flexible molecular structure. DR is defined as

$$DR = rac{f_{slv} - f_{
holm}}{f_{slv}}$$
 (1)

where f_{slv} and f_{plm} are the drag coefficients in the solvent (suspending liquid) and polymer solution, respectively, while each drag coefficient is defined as

$$f = \frac{\tau}{\frac{1}{2}\rho U_{moy}^2} \tag{2}$$

where τ is the shear stress, Umoy the mean velocity and ρ the fluid density [12]. In the literature, authors generally measure the shear stress at solid walls in the water

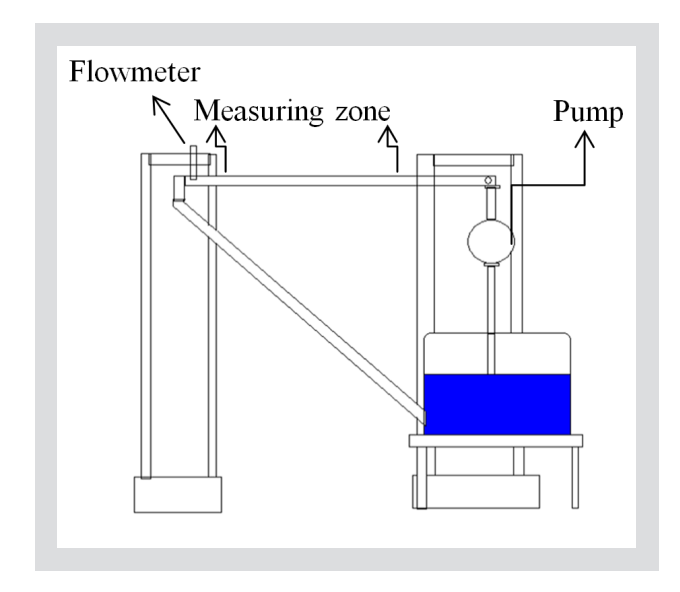


Figure 1: Experimental apparatus.

and solution and derive DR by the use of Equations 1 and 2. To date, experimental measurement of shear stress has used multicomponent single point Laser Doppler Velocimetry (LDV) [13–16], and instantaneous planar maps of the velocity field using Particle Image Velocimetry (PIV) [17 – 20]. The measurements provided by these techniques are reliable and accurate. Unfortunately, the equipment is costly and suitable only for laboratory experiments done in transparent pipes. The aim of the present work is to initiate the development of a new method for measuring DR in dilute polymer solutions that could be used in industrial conditions (e.g. in an opaque pipeline) as it would be based on the measurement of inherent triboelectricity generated in flowing liquid. The only instrumentation required is a multimeter and a flowmeter.

The triboelectricity phenomenon is the generation of electric current by friction between two objects that can be two solids (e.g.: a metal with a metal, a metal with an insulator (non-ionic or with mobile ions), an insulator with an insulator (with mobile ions present or both non-ionic)) [21 – 25]. Also, triboelectricity can occur in a contact between a liquid and a solid. In the past, it was thought that the triboelectricity effect or charge transfer between two materials in friction would occur only when the liquid rubbing against the tube surface was slightly conductive [26-29]. Under these conditions, triboelectricity should depend on the electronaffinity of the fluid and the solid wall with which it is in contact. However, considering that charge transfers derive from the extracting of electrons by the friction of the liquid on the solid wall, Ravelo et al. [30-31] revisited the tribology concept and proposed a hydroelectric model for a Newtonian liquid even if this liquid is insulating. Knorr [32] presents analogies between triboelectricity occurring at fluid flow/solid interface and streaming current/potential phenomena that can be described as follows: At the contact between the aqueous liquid and the pipe, a physico-chemical phenomenon creates a charge separation known as "electrical

double layer" which polarizes the liquid/solid interface. lons of one sign appear on the solid surface while ions of the opposite sign are distributed in the liquid in two layers. Some of these counterions accumulate in an immobile layer (the Stern layer) close to the surface of the solid. The remaining counterions along with other electrolyte ions, form the Gouy-Chapman layer that extends into the electrolyte solution. The total interfacial region is electrically neutral while the distinction between mobile and immobile ions is responsible for several phenomena known as electrokinetic phenomena. If the aqueous solution is put in flow inside the pipe, for example with the help of a pump or an inclination of the pipe, the ions located in the Gouy-Chapman layer will move with the liquid, while the ions located in the Stern layer will remain static. The origin of the charge separation at the solid/liquid interface is still not yet well understood. Specific adsorption, desorption, corrosion, impurities existing in the liquid, etc. are hypothetical mechanisms involved [33 – 38]. Indeed, both triboelectric effect and streaming current/potential phenomena consist in contact electrification at fluid flow/solid wall interface, meanwhile they are different in that triboelectric effect is caused by rubbing [39], while streaming current/potential is caused by transport [40]. Ravelo's hydroelectric model [30-31] will be presented below and generalized to a liquid obeying the power-law rheological behavior in order to measure the drag reduction in a polymer liquid. Then, an experimental study of the rheology of the polymer solutions used (PEO) and the measurement of drag reduction via triboelectric effect will be presented and the results will be compared to those available in the literature.

2 THE HYDROELECTRIC MODEL OF TRIBOELECTRICITY

2.1 THE MODEL IN A LIQUID

The hydroelectric model of triboelectricity considers the Poiseuille flow of an insulating Newtonian liquid (e.g. tap water) in a cylindrical tube. A hydraulic circuit of this type was designed in the present work and is shown in Figure 1. Recently, it was established by Touchard and his team [33–34] that the system presented in Figure 1 is electrically equivalent to an RC-circuit controlled by a current source, with the asymptotic expression of the maximum voltage given by

$$V_{max} = \frac{Ne\Delta P}{8\pi\sigma\eta} \tag{3}$$

where σ is the conductivity of the tested fluid, $e=1.6\cdot 10^{-19}$ C, and N is the number of electrons caught by the fluid from the pipe. Equation 3 shows that the maximum voltage issued from triboelectricity is proportional to the pressure drop in the pipe. For a Newtonian liquid with dynamic viscosity η , the flow rate Q is given in [41] as:

$$Q = \frac{\pi}{128} \frac{\Delta P}{\eta L} D^4 \tag{4}$$

where L is the tube length, D its diameter and ΔP is the pressure drop. Equations 3 and 4 show that, for the Newtonian liquid used as solvent in this case (subscript 'slv'), the maximum voltage of triboelectricity is proportional to flow rate according to:

$$V_{slv} = \frac{16NeL}{\pi^2 D^4 \sigma} Q \tag{5}$$

while the shear stress for a Newtonian fluid is defined by $\tau_{\rm slv}$ = $\eta\dot{\gamma}$ with

$$\dot{\gamma} = \frac{4Q}{\pi R^3} \tag{6}$$

Using Equations 5 and 6, the following linear relation is derived between shear stress and triboelectricity voltage for a Newtonian fluid

$$\tau_{slv} = \frac{4\eta\pi\sigma R}{NeL} V_{slv} \tag{7}$$

In the next section the previous hydroelectric model will be extended to a polymer solution in order to derive drag reduction.

2.2 DRAG REDUCTION IN A POLYMER SOLUTION

The introduction of a small quantity of a polymer into a liquid can modify its rheological behavior. Notably, increasing the rate of strain decreases the viscosity. Such rheological behavior, known as a pseudoplastic or shear-thinning behavior, can be described by a semiempirical law such as Spriggs law, Carreau's law or hyperbolic tangent law [42]. Meanwhile, the power law is more generally used in modeling than these semi-empirical laws. Indeed, despite its lack of relevance to reality at low shearing rates, the power-law model [43] generally leads to satisfactory approximations and allows analytical resolution. If τ denotes the stress tensor,

 $\dot{\epsilon}$ the straining rate tensor, I_d the unit tensor, K the liquid consistency, m the power-law index, and p the pressure field, the power-law equation of state is written

$$\tau = -\rho I_d + K \hat{\epsilon}^m \tag{8}$$

Considering the axial Poiseuille flow in the tube of Figure 1, with velocity field v(o,o,w(r)) in a (r,θ,z) cylindrical coordinate system and pressure drop ΔP , this is governed by the equation of conservation of the momentum which is written

$$div\tau = -gradp + Kdiv\dot{\varepsilon}^m$$
(9)

while the continuity equation is identically satisfied. Equation 9 can be solved analytically and gives the following axial velocity

$$w(r) = \frac{m}{m+1} \left(\frac{1}{2K} \frac{\Delta P}{L} \right)^{1/m} R^{1+1/m} \left[1 - \left(\frac{r}{R} \right)^{1+1/m} \right]$$
 (10)

The flow rate is derived from Equation 10 in the form

$$Q = 2\pi \int_{0}^{R} w(r)r dr = \pi \frac{m}{3m+1} \left(\frac{1}{2K} \frac{\Delta P}{L} \right)^{1/m} R^{3+1/m}$$
(11)

Introducing Touchard's formula given by Equation 3 into the previous formula for flow rate, we obtain the following equation for the hydroelectric characteristic of the polymer solution

$$V_{plm} = \frac{N_{plm}e}{4\pi\sigma_{plm}} \times \frac{L}{R^{t+3m}} \left(\frac{3m+1}{m\pi}\right)^m Q^m$$
(12)

where subscript 'plm' refers to the polymer solution. From the equation of state, the shear stress in a polymer solution is given by $\tau_{\text{plm}} = K \dot{\gamma}^{\text{m}}$ with $\dot{\gamma} = (3m+1)Q/(m\pi R^3)$ Using the above equations, the following linear relation is obtained relating the shear stress and the triboelectric voltage for a pseudoplastic fluid

$$\tau_{plm} = \frac{4\pi\sigma_{plm}KR}{N_{plm}eL}V_{plm} \tag{13}$$

In the equation of state of a pseudoplastic fluid given by Equation 8, Newtonian behavior is obtained for m = 1

while consistency is equal to dynamic viscosity. We can see that shear stress in water can be obtained from Equation 13. Using the definition of DR given by Equations 1 and 2 and the expressions of shear stress in Newtonian and pseudoplastic fluids given by Equation 7 and 13, respectively, we obtain the following expression for DR. For given flow rate and polymer concentration, drag reduction can then be derived and we see that it is determined by the measurement of the relative triboelectricity in the polymer and solvent,

$$DR = 1 - \frac{\sigma_{plm}}{N_{plm}} \frac{N_{slv}}{\sigma_{slv}} \frac{K}{\eta} \frac{V_{plm}}{V_{slv}}$$
(14)

Let S_{slv} and S_{plm} denote the slopes of the hydroelectric characteristics in a Newtonian fluid (given by Equation 5) and in a pseudoplastic fluid (given by Equation 12). The σ/N ratios appearing in Equation 14 are derived from S_{slv} and S_{plm} , respectively. Finally, we obtain the following formula for DR in a polymer solution.

$$DR = 1 - \frac{S_{slv}}{S_{plm}} \frac{\pi R^3}{(\pi R^3)^m} \frac{1}{4} \left(\frac{3m+1}{m}\right)^m \frac{K}{\eta} \frac{V_{plm}}{V_{slv}}$$
(15)

3 EXPERIMENTAL STUDY

In this section, the polymer solution is characterized using rheometry. Drag reduction is measured in relation to PEO concentration using the hydroelectric characteristics.

3.1 RHEOLOGICAL CHARACTERIZATION OF DILUTE POLYETHYLENE OXIDE SOLUTIONS (PEO)

The polymer solutions used were prepared by dispersing a pre-mixture of PEO powder (Aldrich, $8 \cdot 10^6$ g/mol) with isopropyl alcohol in water. The composition of the solvent is 95 % tap water and 5 % isopropyl alcohol. The PEO solutions can be characterized using a microchannel pressure driven flow [44] or a rotating rheometer. In this case, rheometry tests were brought out using an AR2000 Rheometer (TA Instruments), for different concentrations of PEO. The results presented in Figure 2 show that the shear viscosity decreases when the shearing rate increases beyond a critical value. Such rheological behavior is called shear thinning and we note that (i) for a low shearing rate up to a certain critical value $\dot{\gamma}$ critical, the viscosity is constant (Newtonian plateau), and (ii) for a high shearing rate, the viscosity

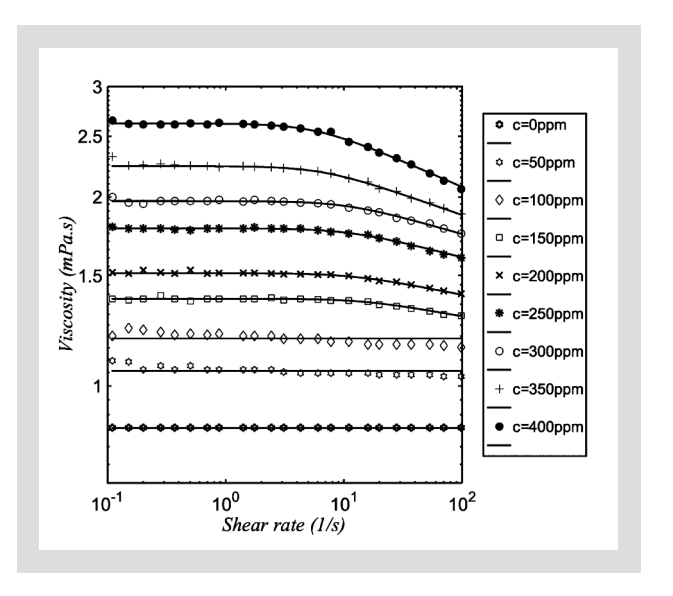


Figure 2: Viscosity of the PEO solutions vs. shear rate for different concentrations.

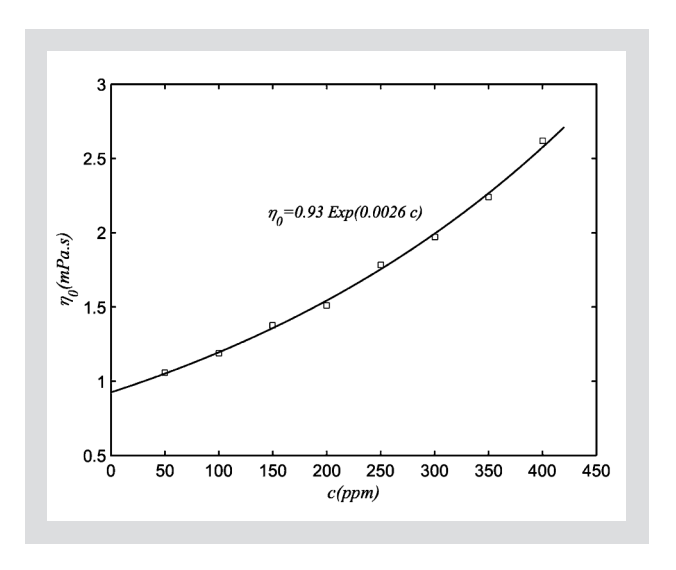


Figure 3: Viscosity of the PEO solutions on the Newtonian plateau versus concentration.

decreases following a power law.

The viscosity can be described by generalized Newtonian model as its equation of state described by Equation 8 can take a Newtonian form $\tau = \eta(\dot{\epsilon})\dot{\epsilon}$ [45–47] but with viscosity depending on shear rate following Ostwald's equation given by $\eta = \eta_o\dot{\gamma}^{m-1}$ when $\dot{\gamma} > \dot{\gamma}_{critical}$ where η_o is the viscosity on the Newtonian plateau or consistency K. The experimental data fitted using Gnuplot software (Fig. 2) provided an exponential variation of consistency versus concentration in PEO noted c with the following expression (Figure 3) K=0.93 x $e^{0.0026c}$ and a linear variation of power-law index versus polymer concentration with the following expression m=0.995-0.0001c. The reduced viscosity is defined by the following relation:

$$\eta_{red} = \frac{\eta_o - \eta_{slv}}{c\eta_{slv}} \tag{16}$$

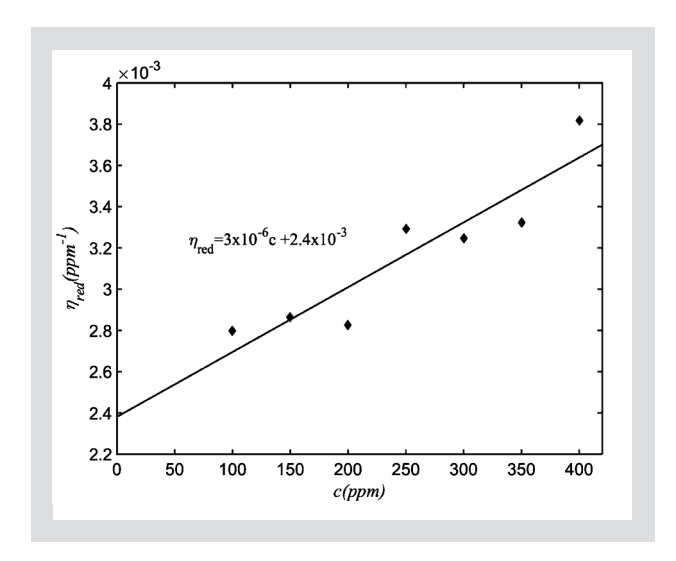


Figure 4: Reduced viscosity of PEO solutions versus concentration.

where $\eta_{\rm slv} = 0.93 \cdot 10^{-3}$ Pa s is the solvent viscosity (95% water + 5% isopropyl alcohol). For 0 < c < 400 ppm, the reduced viscosity increases according to the PEO concentration (Figure 4) following a linear law of the form:

$$\eta_{red} = [\eta_o] + \alpha c \tag{17}$$

where $\alpha = 3 \cdot 10^{-6}$ ppm⁻¹ and $[\eta_o] = 2.4 \cdot 10^{-3}$ ppm⁻¹ is the intrinsic viscosity of a macromolecule of PEO dissolved in the solvent. The recovery concentration is calculated using the Graessley relation:

$$c^* = \frac{o.77}{[\eta_o]} = 321 \, ppm$$
 (18)

For concentrations c, such that $c < c^*$ the PEO solutions are in a dilute regime. Therefore, the PEO solutions tested in this work are diluted because the maximum concentration used is almost equal to the recovery concentration.

3.2 HYDROELECTRIC CHARACTERIZATION

Fig. 5 presents the experimental device designed and built to measure drag reduction via triboelectricity. The pipe (black piece) is 1.20 m long and has a diameter of 10 mm; it is made of steel. The hydraulic circuit is fed by a JAPY JEV 302/303 centrifugal pump (red piece) of 5.8 m³/h maximum flow rate associated with a 50 l tank (green part on Figure 5). The flow rate is measured with the help of a YOKOGAWA Rotameter RAKD that provides a suitable measurable flow range, say 0.1 l/h \leq Q ≤ 8000 l/h. It is mounted in line at the outlet of the pipe and it is equipped with a controller that allows maintaining a constant flow rate irrespective of any process pressure fluctuations. The voltage is measured using an EX 350 EXTECH Instruments Multimeter with a precision of 0.5 % placed on a table, and related to two electrodes introduced in two holes drilled (1 m far from one



Figure 5: Experimental device.

another) in the pipe. The procedure for measuring drag reduction involves 11 steps:

- (1) Take the tube out of the set-up, fill it with tap water and close its 2 outlets. Then, measure the steady static voltage in the water denoted here V_{slv-stat}.
- (2 Reconnect the tube in the set-up and fill the tank with 40 l of tap water. Prepare 8 different test tubes each containing 2 ml of the polymer solution (PEO dissolved in the solvent described in Section 3.1).
- (3) Start the pump and fix the flow rate at 0.2 l/s and then turn on the multimeter. Let the voltage increase until its maximum and steady value, denoted here $V_{slv-meas}$. It is the sum of the triboelectric voltage V_{slv} with the static voltage $V_{slv-stat}$ for the flow rate considered.
- (4) Increase the flow rate to 0.4 l/s and repeat the 3rd step. Further, increase it successively to 0.6, 0.8, 1.0, 1.2, and 1.4 l/s.
- (5) Stop the pump and collect the whole water residing in the tank. Then, pour one test tube of polymer solution and mix with a glass stick.
- (6) Take the tube out of the set-up, fill it with the appropriate quantity of the previous solution contained in the tank and close its 2 outlets. Then, measure the steady static voltage in the polymer solution for the concentration tested and denoted here $V_{plm-stat}$. Return the solution in the tube into the tank and reconnect the tube in the set-up.
- (7) Start the pump and fix the flow rate at 0.2 l/s, then turn on the multimeter. Let the voltage increase until its maximum and steady value, denoted here $V_{plm-meas}$. It is the sum of the triboelectric voltage V_{plm} with the static voltage $V_{plm-stat}$ for the concentration and for the flow rate considered.
- (8) Increase the flow rate to 0.4 l/s and repeat the 7th step. Further, increase it successively to 0.6, 0.8, 1.0, 1.2, and 1.4 l/s.
- (9) Stop the pump and collect the whole water residing in the tank. Pour a second test tube of polymer solution and mix with a glass stick and repeat steps 6 to 8.

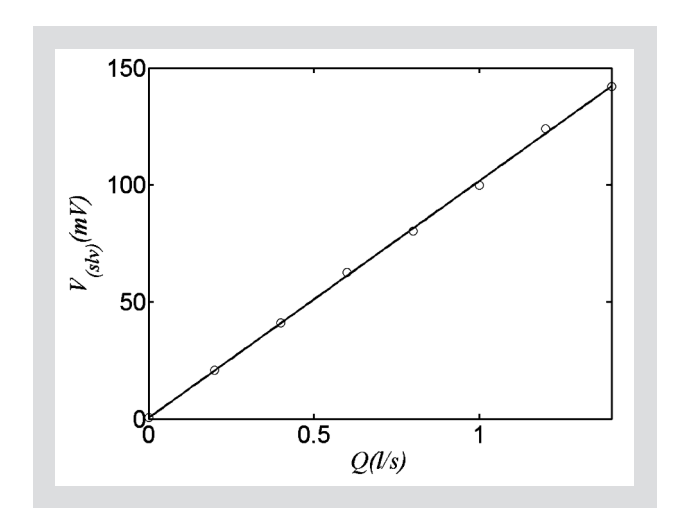


Figure 6: Triboelectric voltage versus flow rate for the solvent.

- (10) Repeat step 9 successively with a 3rd to an 8th test
- (11) Disconnect all devices, empty the solution contained in the tank and clean all the equipments and instruments.

The wet part of the electrodes was 1 mm long so they did not introduce disturbances in the flow. The measurements were repeatable. Table 1 gives the variation of the measured voltage according to the flow rate of the solvent. The hydroelectric characteristic in the solvent derived from Table 1 is written $V_{slv} = S_{slv}Q$ where the slope is obtained from a linear regression, $S_{slv} = 101.2262$ as shown in Figure 6. Similarly, for flowing polymer solution at given flow rate Figure 7 provides the variation of the triboelectric voltage in a polymer solution according to the reduced flow rate Q^m for given PEO concentration. The respective slopes of the hydroelectric characteristics for polymer solutions for assigned concentration with the general form $V_{plm} = S_{plm}Q^m$ are derived from Figure 7 and presented in Table 2.

3.3 DRAG REDUCTION DERIVATION

Using Equation 15, DR can be obtained for assigned polymer concentration where the maximum steady values of the voltage in the solvent and in the polymer

Q (I/s)	V _{slv-mea} (mV)
О	0.51
0.2	20.8
0.4	41
0.6	62.5
0.8	80.2
1.0	99.8
1.2	124
1.4	142

Table 1: Variation of mea-
sured voltage according to
the flow rate of the solvent.

c (ppm)	S _{plm}
50	100.24
100	97.51
150	91.80
200	83.54
250	77.25
300	71.67
350	68.79
400	72.02

Table 2: Variation of the slope of hydroelectric characteristics of PEO solutions for given concentration.

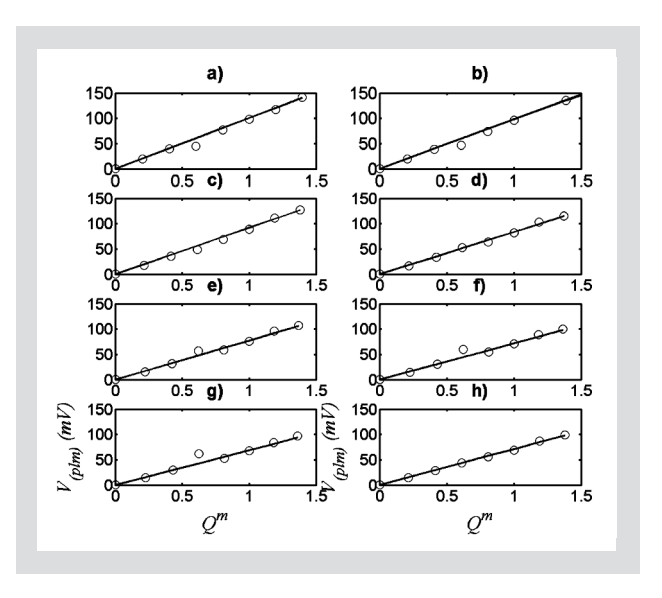


Figure 7: Variation of triboelectric voltage according to reduced flow rate for different concentration of PEO solution: a) c = 50 ppm, b) c = 100 ppm, c) c = 150 ppm, d) c = 200ppm, e) c = 250 ppm, f) c = 300 ppm, g) c = 350 ppm, and h) c = 400 ppm.

 V_{slv} and V_{plm} are given in Figures 6 and 7, respectively. The slopes of the hydroelectric characteristics in the solvent and in the polymer solutions and triboelectric voltage are given by $S_{slv}=101.2262$ and in Table 2, respectively. Figure 3 gives the consistency K of the polymer solution for concentration c and the solvent viscosity for c=0. For all the flow rates tested, the variation of DR against polymer concentration follows a similar shape as in Figure 8 which is obtained for Q=1.4 l/s, where drag reduction reaches its maximum value in the experiment. Notably, DR increases with polymer concentration for c<250 ppm and tends towards saturation for 250 ppm c<400 ppm.

4 DISCUSSION AND CONCLUSIONS

4.1 DISCUSSION

An important issue to discuss in this work is the non-zero voltage measured in static liquid (solvent or polymer solutions) contained in the tube and this is not the case when measured in an open vessel. Indeed, the tube

Q (1/s)	V _{plm} (mV)	$\dot{\gamma}$ (1/s)	Re	DR (%)
0.2	15.3	2040.8	16399	2.16
0.4	29.0	4081.6	31354	7.05
0.6	42.9	6122.3	45807	10.18
0.8	52.9	8163.1	59945	13.84
1.0	62.9	10204	73852	17.9
1.2	73.4	12245	87578	22.85
1.4	80.4	14285	101160	26.24

Table 3: Triboelectric voltage, shear rate, Reynolds number and drag reduction for c = 400 ppm for flow rates lying in the range 0.2 l/s < Q < 1.4 l/s.

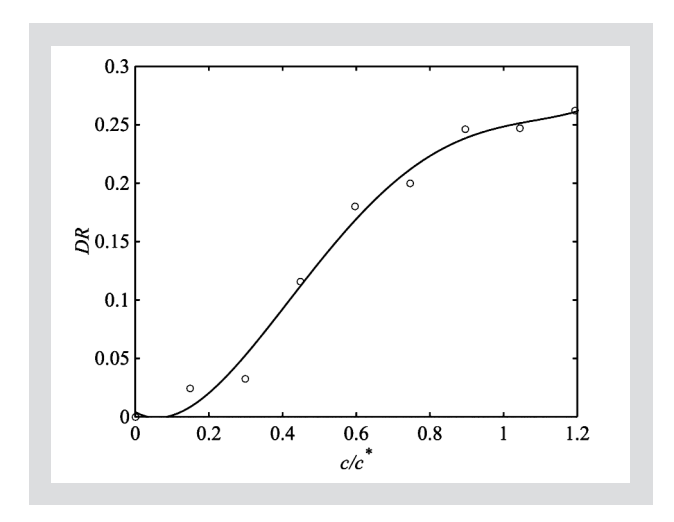


Figure 8: Drag reduction in PEO solution according to polymer concentration.

plays the role of an antenna that transmits to the contained liquid, the electromagnetic waves (mobile phone, etc.) propagating in the room. To cancel them and get zero voltage in static liquid, the measurement must be brought out in a Faraday cage. In this case, the voltage measured in static liquid was substracted from the voltage measured in flow in order to get the triboelectric voltage, i.e. the voltage due to friction. As stated in previous sub-section, for given flow rate, DR increases versus polymer concentration and tends to a plateau (as shown in Figure 8). To explain this property, it is suggested that the polymer chains are stretched by shear and the induced laminarization of the flow is increased by a higher concentration in polymer. Meanwhile for 250 ppm < c < 400 ppm this effect is competed by the chains interactions, therefore, DR tends to a plateau in that range of concentration. Such results agree qualitatively with those existing in literature [48 – 50].

Moreover, for given concentration, DR increases against flow rate with a similar shape, so only the graph for Q = 1.4 l/s where DR is at its maximum is presented. The increasing of drag reduction versus flow rate is shown in Table 3, for c = 400 ppm which is the concentration where DR is maximal. In Table 3 also important dynamic flow characteristics such as shear rate and Reynolds number are calculated. Here, the shear rate is given by

$$\dot{\gamma} = \frac{\left(3m+1\right)Q}{m\pi R^3} \tag{19}$$

while the Reynolds number Re is defined by $Re = U_{moy}D/\nu$ where the mean velocity U_{moy} is given by $U_{moy} = Q/A$ with $A = \pi R^2$. The fluid kinematic viscosity ν and ρ the fluid density are given by $\nu = \eta/\rho$ and $\rho = \rho_{\rm slv}(1+\epsilon)$. The fluid dynamic viscosity η is given by $\eta = \eta_0 \dot{\gamma}^{\rm m-1}$ and the solvent density is equal to $\rho_{\rm slv} = 0.982 \cdot 10^3$ kg m⁻³. Table 3 shows that DR increases with Re. This result is due to a better alignment of the polymer chains with increasing Re. An important issue revealed by Table 3 is

the high values of shear rate and Reynolds number as well. Such values are due to the high values of flow rate and diameter of the tube and that order of magnitude has been operated in literature for DR measuring [48, 51–53]. To investigate drag reduction at high shear rates is important for industrial applications where for instance in pipelines, pipe diameter and flow rate can have higher values.

The corresponding values of shear stress are much higher than those operated in rheometry tests (Figure 2). Indeed, in rotating rheometry, the rheograms are generally presented up to $\dot{\gamma}=100~\text{s}^{-1}$ because for higher shear rate ($\dot{\gamma}=130~\text{s}^{-1}$ in this case), instabilities occur in the form of vortices making the shear stress diverge and the measurement meaningless. Meanwhile, the rheological behavior stated at low shear rate remains valid at high shear rate. Rheometry at high shear rate can be processed using an extensional rheometer [54] and it is noted that at high shear rate, viscosity does not collapse to zero, but tends asymptotically to solvent viscosity [17].

4.2 CONCLUSIONS

To measure drag reduction in dilute polymer solution, the existing methods perform well under laboratory conditions. In this work, we developed a new method that can be used in real conditions, say in opaque and long tubes. The polymer tested was PEO (Polyethylene oxide). To characterize the PEO solutions, rheograms showed that the fluids tested have a pseudoplastic behavior and the model parameters were obtained. Then, an experimental set-up was designed and built that aimed to make a hydroelectric characterization of PEO solutions. The voltage was measured in static solvent and polymer solution. Moreover, in static solution, no variation of the voltage was detected with increasing polymer concentration in the range tested. In flow, triboelectric voltage is due to friction of liquid (solvent or polymer solution) on pipe wall. It was plotted vs. flow rate in the solvent and reduced flow rate in the polymer solutions and the respective linear characteristics were plotted. A model developed in this work gives the drag reduction from the slopes of these characteristics, the triboelectric voltages, the rheological characteristics of the solvent and the polymer solution tested and the pipe diameter as well. It was found that for given flow rate drag reduction increases with polymer concentration for c < 250 ppm and tends toward saturation for 250 ppm < c < 400 ppm. Moreover that variation of drag reduction against concentration is similar for all flow rates tested. While, for given concentration, drag reduction increases with flow rate and is maximum for Q =1.4 l/s in this study. These results agree qualitatively with those existing in literature.

REFERENCES

- [1] Ahmad A, Nsom B, Decruppe JP: Slope effect on core-annular flow, Rheol. Acta 50 (2011) 945 954.
- [2] Truong VT: Drag reduction technologies. Maritime Platforms Division, Aeronauical and Maritime Research Laboratoy, Defence Science and Technology Organization (DSTO), Report N° DSTO-GD-0290, Department of Defence, Victoria, Australia (2001).
- [3] Krope A, Krobe J, Lipus LC: A model for velocity profile in turbulent boundary layer with drag reducing surfactants, Appl. Rheol. 15 (2005) 152–159.
- [4] Dosunmu IT, Shah SN: Steady shear and dynamics properties of drag reducing surfactant solutions, Appl. Rheol. 25 (2015) 12539.
- [5] Mik V, Myska J, Chara Z, Stern P: Durability of a drag reducing solution, Appl. Rheol. 18 (2008) 12421.
- [6] Roy A, Larson RG: A mean flow model for polymer and fiber turbulent drag reduction. Appl. Rheol. 15 (2005) 370-389.
- [7] Ge W: Turbulent drag reduction by surfactant additives, Appl. Rheol. 23 (2013) 84.
- [8] Nsom B. (1994): Computation of drag reduction in fiber suspensions, Fluid Dyn. Res. 14 (1994) 275 288.
- [9] Choi HJ, Kim CA, Sohn JI, Jhon MS: An exponential decay function for polymer degradation in turbulent drag reduction, Polym. Deg. Stab. 69 (2000) 341–346.
- [10] Shefty AM, Solomon MJ: Aggregation in dilute solutions of high molar mass poly (ethylene) oxide and its effect on polymer turbulent drag reduction, Polymer 50 (2009) 261–270.
- [11] Virk PS: Drag reduction fundamentals, AIChE J. 21 (1975) 625–656.
- [12] Bahlouli MI, Bekkour K, Benchabane A, Hemar Y, Nemdili A: The effect of temperature on the rheological behavior of polyethylene oxide (PEO) solutions, Appl. Rheol. 23 (2013) 13435.
- [13] Willmarth WW, Wei T, Lee CO: Laser anemometer measurements of Reynolds stress in a turbulent channel flow with drag reducing polymer additives, Phys. Fluids 30 (1987) 933–935.
- [14] Tiederman WG: The effect of dilute polymer solutions on viscous drag and turbulence structure, in Structure of Turbulence and Drag Reduction, Gyr A (Ed.), Springer, Berlin (1990) 187–200.
- [15] Den Toonder JMJ: Drag reduction by polymer additives in a turbulent pipe flow: Laboratory and numerical experiments, Ph.D. thesis, Delft University of Technology, Delft, The Netherlands (1995).
- [16] Warholic MD, Schmidt GM, Hanratty TJ: The effect of drag reducing surfactant on a turbulent velocity field, J. Fluid Mech. 388 (1999) 1–20.
- [17] Ptasinski PK, Nieuwstadt FTM, van den Brule BHAA, Hulsen MA: Experiments in turbulent pipe flow with polymer additives at maximum drag reduction, Flow. Turbul. Combust. 66 (2001) 159–182.
- [18] Warholic MD, Heist DK, Katcher M, Hanratty TJ: A study with particle-image velocimetry of the influence of drag-reducing polymers on the structure of turbulence, Exp. Fluids 31 (2001) 474 483.
- [19] White CM, Somandepalli VSR, Mungal MG: The turbu-

- lence structure of drag reduced boundary layer flow, Exp. Fluids 36 (2004) 62–69.
- [20] Hou Y, Somandepalli, VSR, Mungal MG: Streamwise development of turbulent boundary layer drag reduction with polymer injection, J. Fluid Mech. 597 (2007) 31 66.
- [21] Williams MW: Triboelectric charging of insulating polymers-some new perspectives, AIP Adv. 2 (2012) 010701.
- [22] Williams MW: Triboelectric charging in metal-polymer contacts—How to distinguish between electron and material transfer mechanisms, J. Electrostatics 71 (2013) 53–54.
- [23] Williams MW: Triboelectric charging of insulators Mass transfer versus electrons/ions, J. Electrostatics 70 (2012) 233 234.
- [24] Williams MW: What creates static electricity, Amer. Sci. 100 (2012) 316–323.
- [25] Williams MW: The increasing role of Chemistry in understanding triboelectric charging of insulating materials A paradigm shift, Phys. Sci. Int. J. 5 (2015) 88 92.
- [26] Henry PSH: Survey of generation and dissipation of static electricity, Brit. J. App. Phys., Suppl. 2 (1953) S6.
- [27] Henniker J: Triboelectricity in polymers, Nature 196 (1962) 474.
- [28] Sakaguchi M, Kashiwabara H: A generation mechanism of triboelectricity due to the reaction of mechanoradicals with mechanoions which are produced by mechanical fracture of solid polymer, Colloid Polym Sci. 270 (1992) 621–626.
- [29] SAE International: Minimization of electrostatic hazards in aircraft fuel systems, Aerospace Information Report, Air 1662, Rev. A (1998).
- [30] Ravelo B, Duval F, Kane S, Nsom B: Demonstration of the triboelectricity effect by flow of liquid water in the insulating pipe, J. Electrostatics 69 (2011) 473 478.
- [31] Ravelo B, Nsom B, Cozien R, Latrache N, Durand B, Eyanga CE: Proof of existence of triboelectricity with liquid water. Actes des 26èmes Journées Int. Francophones de Tribologie, Mines ParisTech, Presses des Mines, Mulhouse (France).
- [32] Knorr N: Squeezing out hydrated protons: Low-frictional energy triboelectric insulator charging on a microscopic scale, AIP Adv. 1 (2011) 022119.
- [33] Paillat T, Touchard G, Bertrand Y: Capacitive sensor to measure flow electrification and prevent electrostatic hazards, Sensors 12 (2012) 14315 14326.
- [34] Paillat T, Morin G, Touchard G, Bertrand Y, Moreau O, Tanguy A: Electrostatic hazard in high power transformers: Analyze of ten years of the capacitive sensor, Proc. ESA/IEEE-IAS/IEJ/SFE Joint Conf. Electrostatics, Cambridge, Canada (2012) 12–14.
- [35] Galembeck F, Burgo TAL, Balestrin LBS, Gouveia RF, Silva CA, Galembeck A: Friction, tribochemistry: Recent progress and perspectives, Roy. Soc. Chem. Adv. 4 (2014) 64280 64298.
- [36] McCarthy LS, Whitesides GM: Electrostatic charging due to separation of ions at interfaces: Contact electrification of ionic electrets, Angew. Chem. Int. Ed. 47 (2008) 2188–2207.
- [37] Paillat T, Morea O, Cabaleiro JM, Perisse F, Touchard G: Electrisation par écoulement: Modélisation électrique, J. Electrostatics 64 (2006) 485–491.

- [38] Olthuis W, Schippers B, Eijkel J, van der Berg A: Energy from streaming current and potential, Sensors Actuators B 111 112 (2005) 385 389.
- [39] da Silva ETSG, Santhiago M, de Souza FR, Coltro WKT, Kubota LT: Triboelectric effect as a new strategy for sealing and controlling the flow in paper-based devices, Lab. Chip 15 (2005) 1651–1655.
- [40] van der Heyden FHJ, Stein D, Dekker C: Streaming currents in a single nanofluidic channel, Phys. Rev. Lett. 95 (2005) 116104.
- [41] Monin AS, Yaglom AM: Statistical fluid mechanics, Vol. 1, Lumley JL (Ed.), The MIT Press, Cambridge (1976).
- [42] Agassant JF, Avenas P, Sergent JP. La Mise en forme des matières plastiques, Approche thermomécanique, Lavoisier Technique et Documentation, Paris (1989).
- [43] Ostwald W: Über die Geschwindigkeitsfunktion des Viskosität disperser Systeme, Kolloid Z. 36 (1925) 99 117.
- [44] Bandulasena HCH, Zimmerman WB, Rees JM: Rheometry of non-Newtonian polymer solution using microchannel pressure driven flow, Appl. Rheol. 20 (2010) 55608.
- [45] Nsom B, Ravelo B, Ndong W: Flow regimes in viscous horizontal dam-break flow of clayous mud, Appl. Rheol. 18 (2008) 43577.

- [46] Di Federico V, Malavasi S., Cintoli: Viscous spreading of non-Newtonian gravity currents on a plane, Meccanica 41 (2006) 207 217.
- [47] Ng CO, Mei CC: Roll waves on a shallow layer of mud modelled as a power-law fluid, J. Fluid Mech. 263 (1994) 151–183.
- [48] Sharma RS, Seshadri V, Malhotra RC: Drag reduction in dilute fiber suspensions: Some characteristic aspects, Chem. Eng. Sci. 34 (1979) 703–713.
- [49] Malhotra JP: Turbulent drag reduction by polymer-fiber mixtures, J. Appl. Polym. Sci. 33 (1987) 2467–2478.
- [50] Kim HT, Kline SJ, Reynolds WC: The production of turbulence near a smooth well in a turbulent boundary, J. Fluid Mech. 50 (1971) 133 160.
- [51] Kale DD, Metzner AB: Turbulent drag reduction in dilute fiber suspension: Mechanistic considerations, AIChE J. 22 (1976) 669 – 674.
- [52] Radin J, Zakin JL, Patterson GK: Drag reduction in solidfluid systems, AIChE J. 21 (1975) 358 – 371.
- [53] Vaseleski RC, Metzner AB: Drag reduction in the turbulent flow of fiber suspensions, AIChE J. 20 (1974) 301–306.
- [54] Wang X, Gordaninejad F: Study of magnetorheological fluids at high shear rates, Rheol. Acta 45 (2006) 899 908.